Correction of Temperature Estimated from a Low-Cost Handheld Infrared Camera for Clinical Monitoring

Evelyn Gutierrez[1(✉)], Benjamin Castañeda[1], and Sylvie Treuillet[2]

[1] Pontificia Universidad Católica del Perú, Av. Universitaria 1801, San Miguel, Lima, Perú
{egutierreza,castaneda.b}@pucp.edu.pe
[2] Laboratoire PRISME, Polytech, 12 rue de Blois, BP 6744, 45067 Orleans Cedex 2, France
sylvie.treuillet@univ-orleans.fr

AQ1

Abstract. The use of low-cost cameras for medical applications has its advantages as it enables affordable and remote evaluations of health problems; however, the accuracy is a limiting factor to use them. Previous studies indicate that parameters from object position like distance camera-object and angle of view could be used to improve temperature estimation from thermal cameras. Nevertheless, most studies are focused on expensive thermal cameras with good accuracy. In this study, an innovative experimental setup is used to study the errors associated to temperature estimation from a low-cost infrared camera: FlirOne Gen3. In our experiments, the image acquisition is done from multiple point of view (distance camera-object and viewing angles) and by using a thermal camera manipulated by hand. Then, using a regression model, a correction is proposed and tested. The results show that our proposed correction improves the temperature estimation and enhance the thermal accuracy.

Keywords: Temperature correction · Low-cost infrared cameras · Clinical thermal imaging

1 Introduction

Thermographic has the potential as a noninvasive tool to be used in clinical monitoring as noted in some studies: [1–5]. However, accurate estimation of the temperature is sometimes required for using it in clinical settings. Professional infrared cameras have the highest accuracy (around ±1 °C) but they are expensive and hard to manipulate.

In recent years, there have been improvements in IR imaging with portable and low-cost cameras as they are more convenient to be used for remote clinical monitoring [6, 7]. On the other hand, the disadvantage of low-cost cameras is the large errors. Technical specification of low-cost IR cameras like FlirOne Gen3 show accuracy of ±3 °C or ±5%.

Some studies exhibit the possibility to improve temperatures estimation from thermal cameras and recent ones consider low-cost cameras. Curran and al. proposed a correction by using a reference object with known temperature in the field of view of the thermal

J. Blanc-Talon et al. (Eds.): ACIVS 2020, LNCS 12002, pp. 1–9, 2020.
https://doi.org/10.1007/978-3-030-40605-9_11

camera [8]. The proposed correction worked well for various thermal cameras but no significant improvement was found for a low-cost IR camera like FlirOne.

It is known that the accuracy depends on many factors, including the distance of the object, the ambient temperature and the emissivity of the observed material. Theoretical studies [9, 10] and experimental results on human skin [11, 12] indicate that the emissivity decreases significantly when the viewing angle is greater than 60°, i.e. the angle between the optical axis of the camera and the normal to the surface, which leads to inaccurate temperature mapping.

Therefore, some works proposed correction for directional emissivity. Cheng and al. estimated a linear relationship from the calibration of the measurement error due to the viewing angle [13]. Zeise and Wagner used a non-linear least squares optimization minimizing the error of the measured output signals from theoretical models describing emissivity as a function of the viewing angle for known material emissivity class (metal/dielectric) [14]. Arnon and al. proposed a correction for clinical monitoring by thermal images based an empirical second-degree polynomial equation for calibrating the decreasing apparent temperature due to dependency of the skin emissivity on the viewing angle [15]. All the previous methods were tested and used with high end thermal cameras but not with low-cost IR cameras.

The distance between the camera and the object has also been considered. Ting and al. use a Kinect to obtain information on the depth of the image scene and proposed a correction based on it [16]. The correction was tested and accuracy was improved in a low-resolution thermal camera.

In the case of a handheld camera, the shooting protocol cannot be perfectly normalized and the point of view remains approximate. In this paper, we present an experimental setup using only a low-cost camera held in hand to study the variations of thermal measurements induced by the camera point of view. Then, we propose a correction based on a regression model to correct the temperature as a function of the viewing angle and the distance of the camera to object.

The document is organized as follows: Sect. 2 explains the experimental setup; Sect. 3 shows the analysis of absolute errors using a low-cost IR camera; Sect. 4 proposes a methodology for correction; and Sect. 5 presents the results after implementing the proposed correction.

2 Experimental Setup

The low-resolution camera used for the experiments is FlirOne Gen 3 (Flir Systems, Oregon, USA) which according to the specifications has accuracy ± 3 °C or $\pm 5\%$, thermal resolution 80×60 and thermal sensitivity is 150 mK.

To analyze the errors, an experimental setup where the temperature could be measured and controlled is required. This is achieved by utilizing a temperature-controlled stage and a controller with LCD touchscreen from LINKAM (Linkam Scientific Instruments Ltd, Waterfield, Epsom, United Kingdom). The temperature stage has a circular piece of metal in the middle which has 2 cm of diameter. The temperature could be set to any value between -196 °C and 125 °C; and the circular piece of metal will increase its temperature until reaching the desired degrees with an accuracy of less than ± 0.1 °C.

Once the temperature is achieved, the device keeps it for around one hour. The metal piece had a reflective surface which was covered with carbon tape for eliminating reflections.

Additionally, four Aruco Markers are placed around the object of interest (piece of metal) to estimate the camera pose relative to the object. From the pose, we principally consider the distance of the camera from the object and the angle between the optical axis and the normal of the object surface. A label is placed on the side of the device to easily identify the set temperature in the experiments. The experimental setup is presented in Fig. 1.

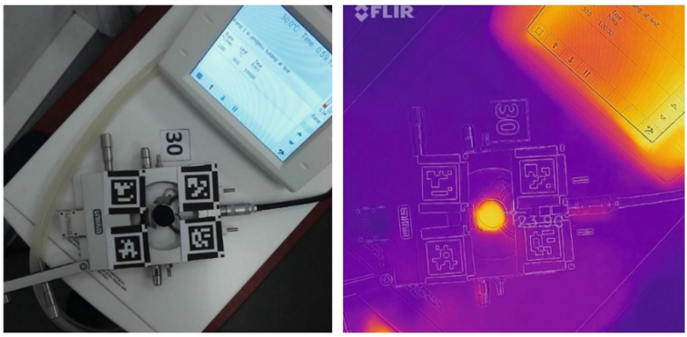

Fig. 1. Experimental set-up: (a) The temperature controlled stage and the Aruko markers; (b) RGB image edges overlaid on Infrared image.

Using this experimental setup and controlling the temperature from 20 to 40 °C, 365 thermal images were captured with FlirOne Gen3 camera connected to an iPad using handheld shooting and varying the point of view. The distance of the camera from the object was varied from 10 to 70 cm and the viewing angle from 0 to 60°. Some examples of image shooting are illustrated in Fig. 2 while Fig. 3 shows illustrates camera poses.

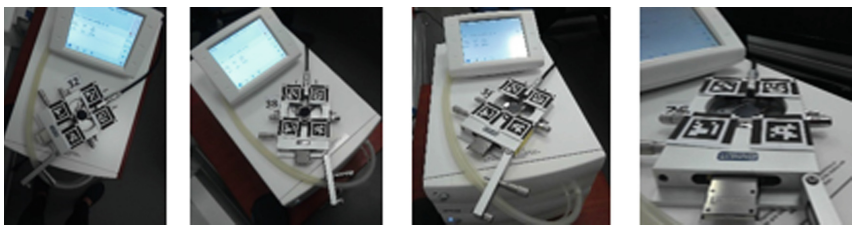

Fig. 2. Sample of images with different points of views.

The temperature has been measured in thermal images using a free package called "thermimage" within statistical software R based on the standard equations used in thermography and described in [17]. The estimation obtained is similar to the one used in

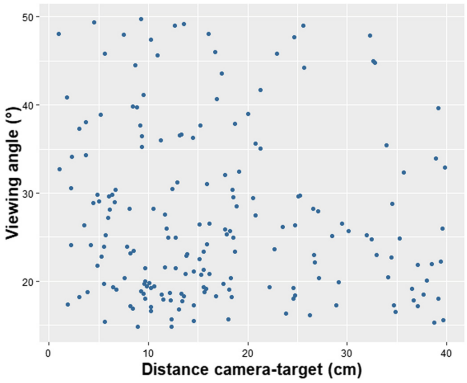

Fig. 3. Different camera poses regarding the distance between camera and target and the angular deviation between the optical axis and the target normal (viewing angle).

commercial Flir software: Tattersall demonstrate that the difference between the estimations from commercial Flir software and the free implementation has mean 0.03 °C and a standard deviation of 0.0312 °C [17].

The temperature estimation takes into account several parameters from the thermal camera which are named Plank constants. The only parameters that have been customized are the following: emissivity, ambient temperature and distance camera-object. For all images, the emissivity was specified to 0.98; ambient temperature to 22 °C; and the distance in centimeters was estimated from the four Aruco markers.

The temperature of the metal plate is measured in the thermal image by calculating the median value in a region of interest (ROI) of 6 × 6 pixels (T_{Est}). The region of interest is illustrated in Fig. 4.

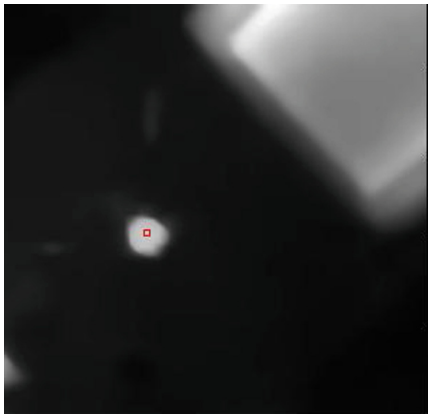

Fig. 4. Thermal image and the ROI of 6 × 6 pixels used to estimate the temperature of metal plate.

3 Analysis of Errors

The difference between the reference temperature (T_{Ref}) and the temperature estimation (T_{Est}) are used to calculate the estimation errors. Figure 5 shows the boxplots of the absolute error at different reference temperatures. The graph suggests a relationship between the absolute error and the reference temperature.

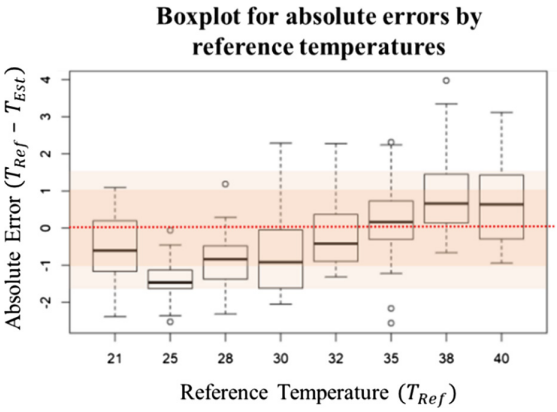

Fig. 5. Boxplot of absolute errors at different reference temperatures.

Similarly, to study the errors regarding the camera position, some plots of the absolute error against the distance and angles are presented in Fig. 6. On the left, the scatterplot shows the relationship between the estimation errors regarding the distance from the camera to the target and, on the right, regarding the viewing angles. A linear relationship can be assumed with the distance but it is not so evident for the angles.

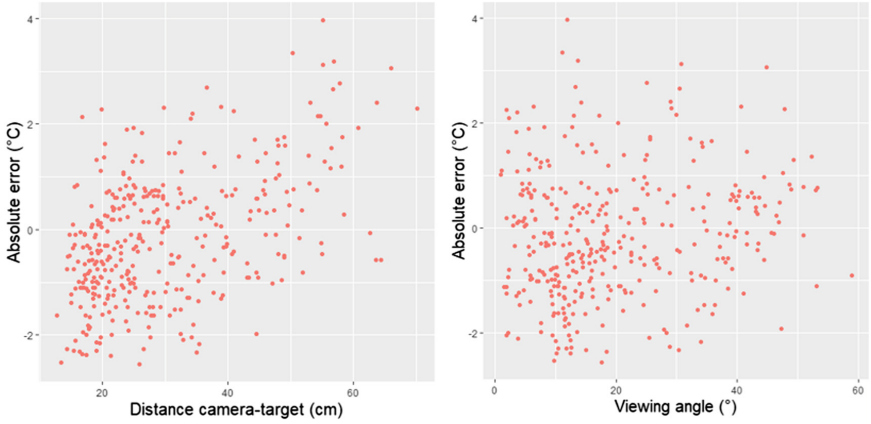

Fig. 6. Scatterplots of the estimation errors against the distances of the camera (left) and viewing angle (right)

Based on these observations, it seems possible to propose a correction of the measured temperature.

4 Proposed Model for Correction

As we want to use the correction for clinical purposes, the dataset used for the proposed correction contains only pictures with temperatures between 30 to 40°; distances between 10 and 50 cm; and angles between 0 to 40°. Using these criteria, a set of 190 images were finally selected.

A regression model is proposed to correct the estimated temperature. This model will be used to estimate reference temperature; however, T_{Ref} will not be used as the response variable. This variable is controlled in the experiments and therefore is not a random variable that could be fitted using regression model. Instead, T_{Est} is used as the response variable and for implementing this model, a methodology used commonly in chemistry for calibration of instruments is used. This methodology is called inverse prediction [18] and it allows to predict the values of the variable of interest: the reference temperature $\left(T_{Ref}\right)$.

In order to define the variables used in the proposed model, a granular analysis of the estimated temperature against distance and angles has been done. In Fig. 7, the estimated temperature is seen as a function of the distances and angles. Each color represents the experiments in a specific controlled temperature. In this figure, a consistent linear relationship between the estimated temperature and the distance could be seen. In contrast, a weaker relationship with the angles is visualized with a second order polynomial relationship. Based on these results, a linear relationship with the distances and a second order polynomial relationship with the angles were considered for the structure of the proposed model.

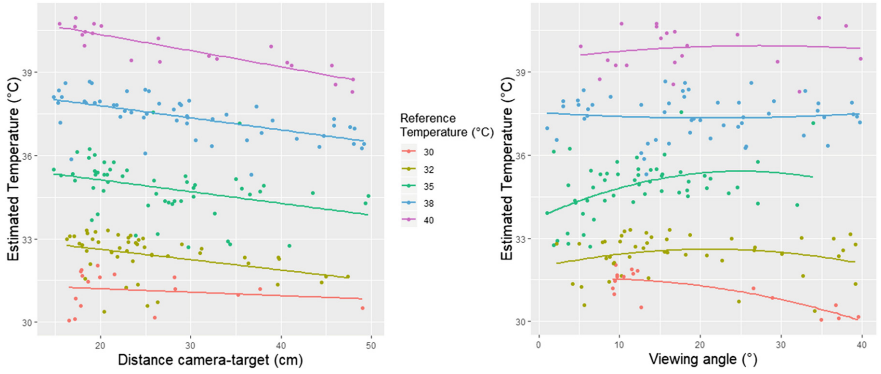

Fig. 7. Scatterplots of the estimated temperature against the distances from camera to object (left) and angle between camera plane and object plane (right).

For validating the proposed model, 5-fold cross validation was used and the Root Mean Squared Error (RMSE) was calculated. The average RMSE obtained in cross

validation after using the proposed model is 0.855. In contrast, the RMSE of the initial temperature estimation was 0.969. This proves that using the proposed model structure, it is possible to reduce estimation errors.

Furthermore, the proposed model was fitted using the whole dataset to obtain the final estimates. Its structure is presented in Eq. (1), and estimated coefficients (β_i) are given in Table 1.

$$T_{Est} = \beta_0 + \beta_1 T_{Ref} + \beta_2 D + \beta_3 A + \beta_4 A^2 + \varepsilon, \tag{1}$$

Where D is the distance of the camera to the temperature controlled target and A is the viewing angle.

Table 1. Estimated beta coefficients for model described in Eq. (1)

Predictors	Estimates	Confidence interval	p-value
Intercept (β_0)	5.051	[3.998–6.988]	<0.001
Reference temp. (β_1)	0.874	[0.823–0.908]	<0.001
Distance (β_2)	−0.042	[−0.059–−0.030]	<0.001
Angle (β_3)	0.065	[0.004–0.102]	0.038
Angle squared (β_4)	−0.002	[−0.002–−0.0001]	0.038
Observations	190		
R2/adjusted R2	0.93/0.928		

Finally, Fig. 8 presents the boxplots without outliers for the absolute error before and after the proposed correction. Before correction, the errors were between −2.56 °C and 2.31 °C while after applying the proposed correction, the errors are between −1.44 °C and 1.66 °C.

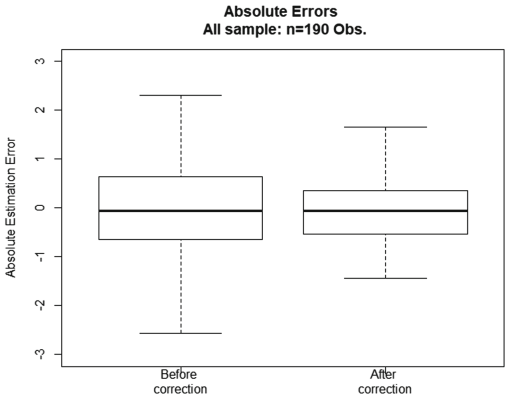

Fig. 8. Boxplot of the absolute errors before and after implementing the proposed correction.

5 Conclusions

Portable and low-cost cameras like FlirOne Gen 3 could have a low accuracy as described in their specifications. Moreover, in the use of clinical applications with handheld camera, the point of view cannot be controlled carefully.

The temperature accuracy depends on point of view and in particular, on the distance of the object and viewing angle. This study shows that it is possible to improve the temperature estimation by using a regression model and inverse prediction. As a result, this could enable improvements in low-cost infrared cameras for being used in clinical measurements.

Future work includes testing the proposed methodology for generalization using another low-cost thermal camera and a larger set of experiments varying environmental conditions (even if the temperature does not vary much indoors with air conditioning). The proposed correction will be used in thermal images of human skin. Finally, we plan to create 3D thermograms for wounds monitoring: corrected thermal information could be overlaid onto 3D models in order to provide accurate healing indexes.

Acknowledgments. This project has received funding from the European Union's Horizon 2020 research and innovation program under the Marie Sklodowska-Curie grant agreement #777661 (STANDUP project).

References

1. Colantonio, S., Pieri, G., Salvetti, O., Benvenuti, M., Barone, S., Carassale, L.: A method to integrate thermographic data and 3D shapes for Diabetic Foot Disease. In: Proceedings of the International Conference on Quantitative InfraRed Thermography (2006)
2. Serbu, G.: Infrared imaging of the diabetic foot. InfraMation **86**, 5–20 (2009)
3. Vilcahuaman, L., et al.: Detection of diabetic foot hyperthermia by infrared imaging. In: 36th Annual International Conference of the IEEE Engineering in Medicine and Biology Society (2014)
4. Fraiwan, L., Alkhodari, M., Ninan, J., Mustafa, B., Saleh, A., Ghazal, M.: Diabetic foot ulcer mobile detection system using smart phone thermal camera: a feasibility study. BioMed. Eng. OnLine **16**, 117 (2017)
5. Alametsä, J., Oikarainen, M., Perttunen, J., Viik, J., Vaalasti, A.: Thermal imaging in skin trauma evaluation: observations by CAT S60 mobile phone. Finnish J. eHealth eWelfare **10**, 192–199 (2018)
6. Bougrine, A., Harba, R., Canals, R., Ledee, R., Jabloun, M.: A joint snake and atlas-based segmentation of plantar foot thermal images. In: Seventh International Conference on Image Processing Theory, Tools and Applications, IPTA (2017)
7. Doremalen, R.V., Netten, J.V., Baal, J.V., Vollenbroek-Hutten, M., Heijden, F.V.D.: Validation of low-cost smartphone-based thermal camera for diabetic foot assessment. Diabetes Res. Clin. Pract. **149**, 132–139 (2019)
8. Curran, A., Klein, M., Hepokoski, M., Packard, C.: Improving the accuracy of infrared measurements of skin temperature. Extrem. Physiol. Med. **4**, A140 (2015)
9. Watmough, D.J., Fowler, P.W., Oliver, R.: The thermal scanning of a curved isothermal surface: implications for clinical thermography. Phys. Med. Biol. **15**, 1–8 (1970)

10. Hejazi, S., Spangler, R.: Theoretical modeling of skin emissivity. In: Proceedings of the Annual International Conference of the IEEE Engineering in Medicine and Biology Society (1992)
11. Lewis, D.W., et al.: Apparent temperature degradation in thermograms of human anatomy viewed obliquely. Radiology **106**(1), 95–99 (1973)
12. Ash, C.J., Gotti, E., Haik, C.H.: Thermography of the curved living skin surface. Mol. Med. **84**, 702–708 (1987)
13. Cheng, T.-Y. et al.: Curvature effect quantification for In-Vivo IR thermography. In: Biomedical and Biotechnology, vol. 2 (2012)
14. Zeise, B., Wagner, B.: Temperature correction and reflection removal in thermal images using 3D temperature mapping. In: Proceedings of the 13th International Conference on Informatics in Control, Automation and Robotics (2016)
15. Arnon, B., Oria, K., Arieli, Y.: Correction of the angular emissivity of human skin for clinical thermal imaging. Imaging Med. **9**(4), 103–108 (2017)
16. Ting, L.P.: Errors in thermographic camera measurement caused by known heat sources and depth based correction. Int. J. Autom. Smart Technol. **6**, 5–12 (2016)
17. Tattersall, G.J.: Thermimage: Thermal Image Analysis, 3 December 2017. http://doi.org/10.5281/zenodo.1069704. R package https://CRAN.R-project.org/package=Thermimage. Accessed 14 Sept 2019
18. Massart, L.M., Vandenginste, B.G.M., Buydens, L.M.C., De Jong, S., Lewi, P.J., Smeyers-Verbeke, J.: Handbook of Chemometrics and Qualimetrics: Part A. Elsevier, Amsterdam (1997)

Author Queries

Chapter 11

Query Refs.	Details Required	Author's response
AQ1	This is to inform you that corresponding author has been identified as per the information available in the Copyright form.	